Peripheral nerve transfers change target muscle structure and function

NEUROSCIENCE

Peripheral nerve transfers change target muscle structure and function

Konstantin D. Bergmeister[1,2], Martin Aman[1,2], Silvia Muceli[3,4], Ivan Vujaklija[3], Krisztina Manzano-Szalai[1], Ewald Unger[5], Ruth A. Byrne[6], Clemens Scheinecker[6], Otto Riedl[1], Stefan Salminger[1,7], Florian Frommlet[8], Gregory H. Borschel[9], Dario Farina[3], Oskar C. Aszmann[1,7]*

Selective nerve transfers surgically rewire motor neurons and are used in extremity reconstruction to restore muscle function or to facilitate intuitive prosthetic control. We investigated the neurophysiological effects of rewiring motor axons originating from spinal motor neuron pools into target muscles with lower innervation ratio in a rat model. Following reinnervation, the target muscle's force regenerated almost completely, with the motor unit population increasing to 116% in functional and 172% in histological assessments with subsequently smaller muscle units. Muscle fiber type populations transformed into the donor nerve's original muscles. We thus demonstrate that axons of alternative spinal origin can hyper-reinnervate target muscles without loss of muscle force regeneration, but with a donor-specific shift in muscle fiber type. These results explain the excellent clinical outcomes following nerve transfers in neuromuscular reconstruction. They indicate that reinnervated muscles can provide an accurate bioscreen to display neural information of lost body parts for high-fidelity prosthetic control.

INTRODUCTION

The motor unit pool of a muscle is precisely aligned during neonatal maturation to the required muscle functionality within a broad range of motions. The coordinated recruitment of motor units is essential for the versatile functions of skeletal muscles (*1*). After reconstructive nerve surgery, muscle force and function are often impaired because of incomplete reinnervation and altered motor unit properties (*2*, *3*). Surgical peripheral nerve transfers can overcome some of these dismal effects by specifically transferring a high-capacity donor nerve (i.e., peripheral nerves with large cognitive control such as the ulnar and median nerves) of a sufficiently large motor neuron pool to an alternate target muscle (*4*, *5*). This is particularly prominent in targeted muscle reinnervation (TMR), where the entire amputated extremity nerves without targets are surgically transferred into single proximal muscles. These nerves physiologically innervate distal muscle groups with high innervation ratios and are transferred to muscles with lower natural innervation density in the amputee's residual stump. Thereby, reinnervated muscles provide bioscreens of neural activity, which can be recorded via electromyography (EMG) for use as a man-machine interface in prosthetic extremity reconstruction (*6*–*9*).

Because of the numerical discrepancy with the original innervation, motor neurons of the donor nerve must compete for the reinnervation of available muscle fibers. Previous studies indicate that transferring multiple donor nerves or reducing the amount of target muscle can lead to hyper-reinnervation, i.e., the reinnervation of a specific muscle fiber population by a higher number of motor neurons (*5*, *10*). We recently found an unexpectedly low number of motor neurons responsible for versatile hand function (*11*); thus, small increments in motor unit density may substantially increase information transfer. This rewiring may, however, lead to significant alterations of the motor unit in terms of structure, function, and protein expression (*6*, *10*), and thus, change the motor unit composition with currently unknown effects. Despite the routine use of nerve transfers, assumptions about the neurophysiological effects on the motor unit can, so far, only be derived from cross-innervation studies that used antagonistic donor nerves. And thus, do not shift to agonistic motor neuron pools of higher innervation density. Furthermore, most of these studies were conducted in hindlimb models that do not well represent the forelimb, as indicated by the poor results of nerve transfers in the lower extremity (*12*).

In this study, we experimentally investigated the effects of high-capacity nerve transfers on all motor unit levels in a rat forelimb model. Similar to clinical applications, the ulnar nerve was transferred to the lateral head of the biceps, instead of its original motor branch. Our results indicate that these nerve transfers do not lead to a loss of muscle force regeneration; however, they determine a donor-specific shift of the muscle fiber type with increased motor unit number. This explains the excellent results achieved after selective distal nerve transfers and supports the use of targeted reinnervation to provide a highly accurate bioscreen to display neural information of lost body parts for high-fidelity prosthetic control.

RESULTS

High-capacity nerve transfer reinnervating a single target muscle

We simulated clinical nerve transfer and TMR procedures to reinnervate a single target muscle by a high-capacity donor nerve in a rat forelimb model. The entire ulnar nerve was microsurgically transferred to the lateral head of the biceps, instead of its original motor branch from the musculocutaneous nerve (Fig. 1). Retrograde labeling identified a total of 280.50 ± 25.87 motor neurons in the high-capacity donor ulnar nerve, which physiologically innervates

[1]CD Laboratory for the Restoration of Extremity Function, Department of Surgery, Medical University of Vienna, Vienna, Austria. [2]Center for Biomedical Research, Medical University of Vienna, Vienna, Austria. [3]Department of Bioengineering, Imperial College London, London, UK. [4]Clinic for Trauma Surgery, Orthopaedic Surgery and Plastic Surgery–Research Department of Neurorehabilitation Systems, University Medical Center Göttingen, Göttingen, Germany. [5]Center for Medical Physics and Biomedical Engineering, Medical University of Vienna, Vienna, Austria. [6]Division of Rheumatology, Clinic for Internal Medicine III, Medical University of Vienna, Vienna, Austria. [7]Division of Plastic and Reconstructive Surgery, Medical University of Vienna, Vienna, Austria. [8]Center for Medical Statistics, Informatics and Intelligent Systems, Section for Medical Statistics, Medical University of Vienna, Vienna, Austria. [9]Division of Plastic and Reconstructive Surgery, The Hospital for Sick Children, Toronto, ON, Canada.
*Corresponding author. Email: oskar.aszmann@meduniwien.ac.at

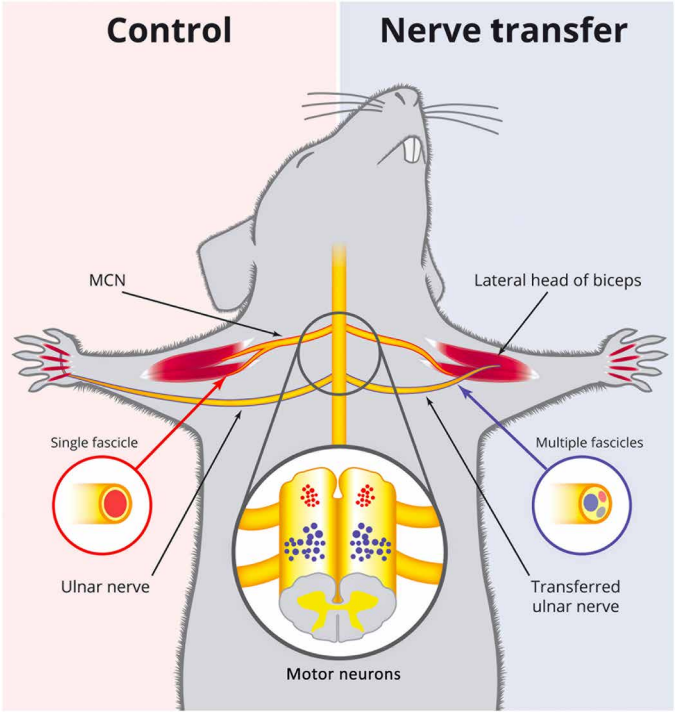

Fig. 1. Experimental nerve transfer model. A high-capacity multifascicular donor nerve originating from a different spinal topography was surgically transferred to selectively reinnervate a single target muscle instead of its original motor branch. The contralateral untreated side was used as control. The nerve transfer successfully reinnervated the target muscle, and no additional reinnervation was observed during dissection or electrophysiological testing. MCN, musculocutaneous nerve.

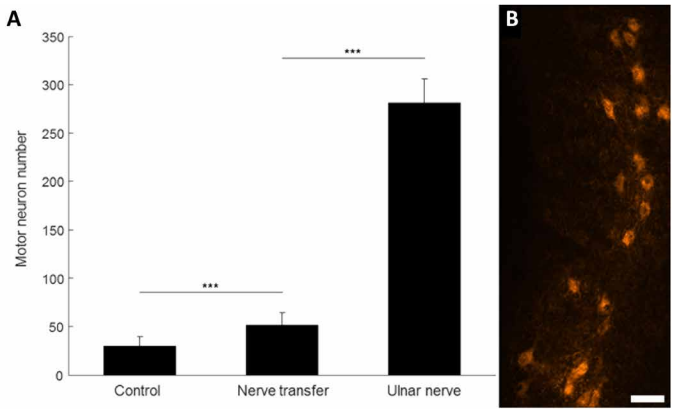

Fig. 2. Structural hyper-reinnervation of the targeted muscle was indicated by retrograde labeling. (**A**) The number of motor units reinnervating the targeted muscle increased significantly (unpaired Student's *t* test, $P = 0.006$), from 29.33 ± 10.01 in control muscles ($n = 6$) to 50.56 ± 13.58 ($n = 9$) by 172.35% at 12 weeks after the nerve transfer. The donor ulnar nerve contained 280.50 ± 25.87 ($n = 6$) motor neurons, but only 18.02% reinnervated the targeted muscle (unpaired Student's *t* test, $P < 0.0001$). ***$P < 0.01$. (**B**) Example of the ulnar nerve's motor neuron column in the spinal cord of a control rat (scale bar, 50 μm; longitudinal section, rat spinal cord).

multiple muscles. These were thereby surgically transferred to a single muscle with a physiological innervation of only 29.33 ± 10.01 motor neurons (Fig. 2). This potentially provided an almost 10-fold increase of motor neurons available for reinnervation.

Twelve weeks after surgery, the donor ulnar nerve successfully reinnervated the biceps' lateral head in all animals. No additional or gross aberrant reinnervation was observed during dissection or electrophysiological testing. Retrograde labeling revealed an average of 50.56 ± 13.58 motor neurons innervating the target muscle after 12 weeks, showing a significant hyper-reinnervation of 172.35% (Fig. 2). This reinnervation represented 18.02% of the available motor neurons from the donor ulnar nerve.

Using confocal and multiphoton microscopy of muscles of Thy1-GFP transgenic rats expressing green fluorescent protein (GFP) in neurons and axons, the remaining axons of motor neurons not innervating the target muscle were identified at the nerve's insertion into the target muscle. Here, they contributed to neuroma-like formations, most likely combined with sensory fibers that did not make target contact (Fig. 3). Hyper-reinnervated muscles qualitatively demonstrated a higher number of axons entering the muscle compared with control. The axonal architecture within targeted muscles showed the typical arborization of axons as they approached the neuromuscular junctions (Fig. 3C), which were identified with red fluorescent staining using α-bungarotoxin targeting antibodies. Even with increased axonal load, axons innervated multiple muscle fibers proximal or adjacent to each other, with polyinnervation of neuromuscular junctions being present in only one animal (Fig. 3, C and D).

Muscle fiber type following reinnervation

Muscle function is determined during neonatal development by motor neuron innervation and subsequent expression of myosin heavy chain (MHC) protein in muscle fibers. To identify the effect of high-capacity nerve transfers on adult muscle fiber populations, we performed muscle fiber analyses on 20-μm cross sections using immunohistochemical staining against MHC subtypes. Control muscle samples of the lateral head of biceps showed a physiological pattern of predominantly fast MHC-IIb fibers, gathering around a core of intermediate MHC-IIa fibers and fewer slow MHC-I fibers (Fig. 4A). Within 12 weeks after surgery, this pattern changed substantially as MHC-IIb fibers were reduced and MHC-IIa fibers and MHC-I fibers were increased (Fig. 4B). This pattern is similar to muscles innervated by the ulnar nerve, for example, the lumbrical muscles of the paw, which almost predominantly consist of MHC-IIa and MHC-I fibers (Fig. 4C). Therefore, the targeted muscle's fiber populations adapted to the physiological properties (needs) of the reinnervating motor neuron pool.

Functional changes in motor unit populations

On the basis of the fundamental structural changes in the target muscle, we expected similar effects on the target muscle's functional properties. We analyzed maximum force, average force per motor unit, and motor unit number in direct comparison to each animal's contralateral extremity. Maximum muscle force was assessed using a force transducer linked to the tendon of the biceps' lateral head and supramaximal stimuli of the transferred ulnar nerve, or motor branch in control muscles. Muscle force progressively regenerated to near-normal levels, which is not typically seen in nerve injuries with complete transection of the nerve (neurotmesis) and is likely the effect of the high number of axons available for reinnervation (Fig. 5, maximum force). This progressive regeneration was similar in the recovery of muscle mass after the initial denervation and subsequent weight loss of the target muscle (Fig. 5, weight).

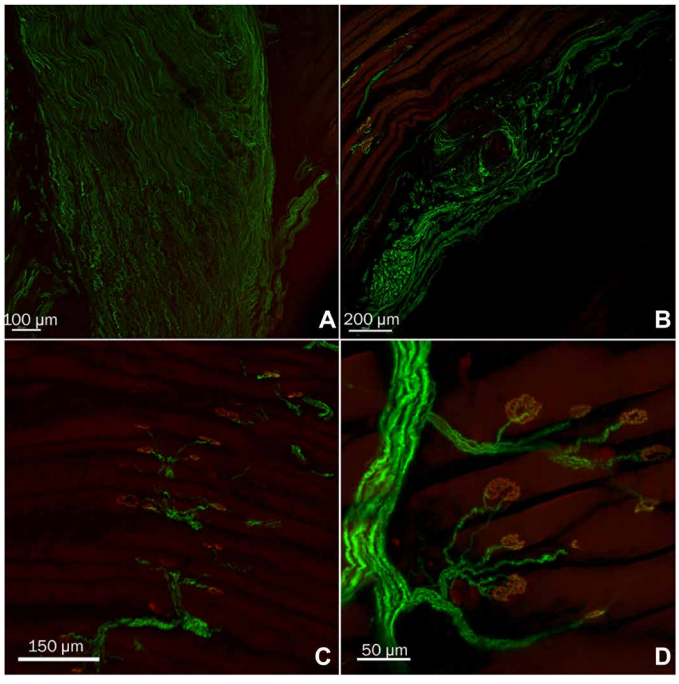

Fig. 3. Confocal and multiphoton imaging of muscular reinnervation after the nerve transfer. (**A** and **B**) The high-capacity donor nerve contained a higher axonal load than the original motor branch. This led to the formation of a neuroma at the muscular insertion point. The typically severe pain or consecutive relieving posture following neuroma formation was not present in any animal. (**C**) The nerve transfer reinnervated the muscle following the route of the original motor branch. Axonal architecture showed the typical arborization of axons as they approached neuromuscular junctions in nerve transfer muscles ($n = 6$). In the six targeted muscles, a total of 2120 neuromuscular junctions were analyzed (353.33 ± 133.55) per animal. Denervated ($n = 1$, 0.16%) or polyinnervated ($n = 17$, 2.79%) neuromuscular junctions were present only in one animal. All other animals did not show any denervated or polyinnervated neuromuscular junction. (**D**) Axons innervated multiple muscle fibers proximal or adjacent to each other. Innervation of neuromuscular junctions by reinnervating axons was confirmed by matching fluorescence expression of axons (green) and neuromuscular junctions (red).

In the course of reinnervation, motor unit number estimates by electrostimulation identified a hyper-reinnervation of the target muscle (Fig. 5, MUNE). Therefore, the higher number of motor neurons identified by retrograde labeling reinnervated stimulable muscle units and elicited their activation within the target muscle, as it was evident in two independent analyses. Hyper-reinnervation therefore provided a high number of motor units (axons) for reinnervation, which innervated most muscle fibers and thereby restored muscle force almost completely. Furthermore, the target muscle was reinnervated by a higher number of motor axons, which led to the formation of smaller muscle units.

Muscle unit fractioning

To investigate the properties of the muscle units following hyper-reinnervation, we used custom-designed high-density epimysial EMG sensors with 48 recording sites placed in the longitudinal axis of the muscle (Fig. 6E). Using crush stimulation of the nerve, we were able to identify single motor units for subsequent analyses of their contractile properties. A total of 100 motor units were detected from the nerve transfer muscles, and 70 were detected for the control side. This difference in identified motor units is likely due to hyper-reinnervation based on the findings from retrograde labeling and motor unit number estimations. The analyses of the propagation velocity of the action potentials along the muscle fibers for the two motor unit populations showed a mean of 2.50 ± 0.86 m/s for the nerve transfer muscle and 2.25 ± 0.75 m/s for the control side (Fig. 6, A and C). The greater conduction velocity after hyper-reinnervation indicated that, on average, the motor units contained fibers with bigger diameters (*13*, *14*). However, the amplitude of the analyzed motor units did not differ between the targeted muscle and the control side (Fig. 6, B and D), suggesting that the number of innervated muscle fibers per muscle units remained similar after the nerve transfer (*15*). Overall, these results suggest that the largest muscle units with greater conduction velocities were fractioned after the nerve transfer so that more motor axons innervated smaller muscle units with larger conduction velocities. Therefore, as the target muscle is hyper-reinnervated by a high-capacity nerve transfer, more motor neurons innervate smaller muscle units, as was also evident from the motor unit number estimates.

DISCUSSION

We demonstrate that target muscles adapt to reinnervation by a larger alternate motor unit pool following surgical nerve transfer. The muscle was hyper-reinnervated by a larger motor neuron pool, which consequently led to smaller muscle units, and muscle fibers adapted to the physiological properties of these reinnervating motor neurons. Therefore, we showed that nerve transfers can be used to rewire target muscles to different motor neuron pools, with subsequent adaptation of the target muscles to the properties of the nerves' original muscles. This structural and functional rewiring can be applied for both biological and prosthetic extremity reconstructions and may help to restore dexterous extremity control (*9*).

Surgical rewiring of motor units

In the upper extremity, coordinated movement is dependent on a precise interplay of multiple muscle groups. Distal muscles have greater innervation ratio than proximal ones. In peripheral nerve transfers or TMR, this sensitive physiological interplay is disrupted, and large motor unit pools of distal muscles are connected to available more proximal target muscles. In our analyses, we have shown that the structural differences between the original motor branch of the target muscle and the transferred nerve did not impair functional regeneration. Instead, substantial hyper-reinnervation of the target muscle was shown in functional electrostimulation and histological assessments. This surplus of motor neurons available for muscle fiber reinnervation was likely responsible for the full recovery of muscle force and muscle weight and the absence of denervated neuromuscular junctions in confocal and multiphoton microscopy. In comparison, direct nerve repairs show a higher number of denervated muscle fibers, as axonal reinnervation is often incomplete across nerve repairs, and thus fewer motor units are available for reinnervation (*2*, *3*). In addition, the absence of polyinnervated neuromuscular junctions suggests that the hyper-reinnervation does not overload the target muscle. Instead, within a short time frame, neuromuscular junctions are successfully reinnervated by the rerouted axons, and the target muscle is highly functional. This high regeneration capacity of the nerve transfer is further enhanced by the short regeneration distance to the neuromuscular junctions. As

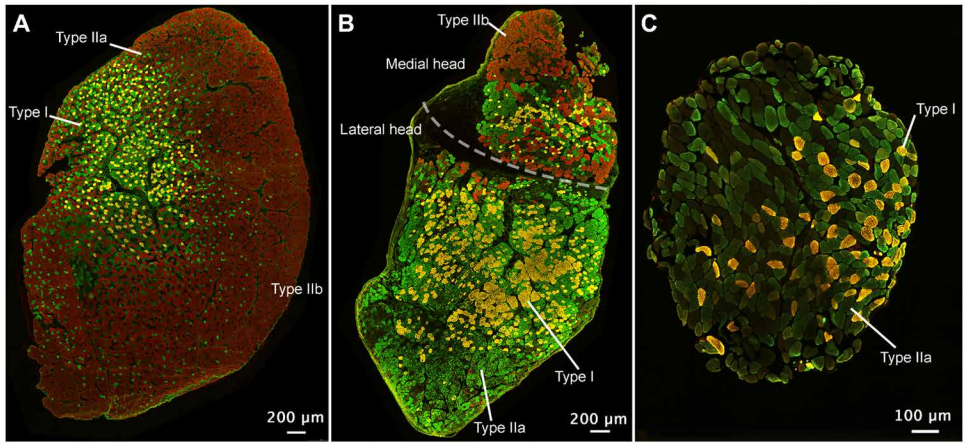

Fig. 4. Nerve transfers changed muscle fiber populations. These were analyzed using immunohistochemistry against MHC proteins. (**A**) Control muscle samples ($n = 10$) of the biceps' lateral head showed predominantly fast MHC-IIb fibers (red; 63.30%, 4445.10 ± 1787.08) gathering around a core of intermediate MHC-IIa fibers (green; 32.63%, 2291.70 ± 995.99) and fewer slow MHC-I fibers (golden; 4.07%, 285.80 ± 204.51). (**B**) After the nerve transfer, populations changed substantially as MHC-IIb fibers (red; 46.44%, 2622.30 ± 953.35) were reduced, while MHC-IIa (green; 44.84%, 2531.70 ± 1566.45) and MHC-I fibers (golden; 8.72%, 492.10 ± 313.53) increased ($n = 10$). Above the dashed line is the medial head of the biceps whose innervation remained unchanged, containing mainly MHC-IIB fibers (red). The overall number of muscle fibers between the nerve transfer and control muscles did not statistically differ at 12 weeks [analysis of covariance (ANCOVA), $P = 0.43$], suggesting no significant muscle fiber loss due to denervation. (**C**) Lumbrical muscles innervated by the donor ulnar nerve physiologically show a similar fiber pattern as the biceps after the nerve transfer (B), with exclusively slow MHC-I and intermediate MHC-IIa fibers.

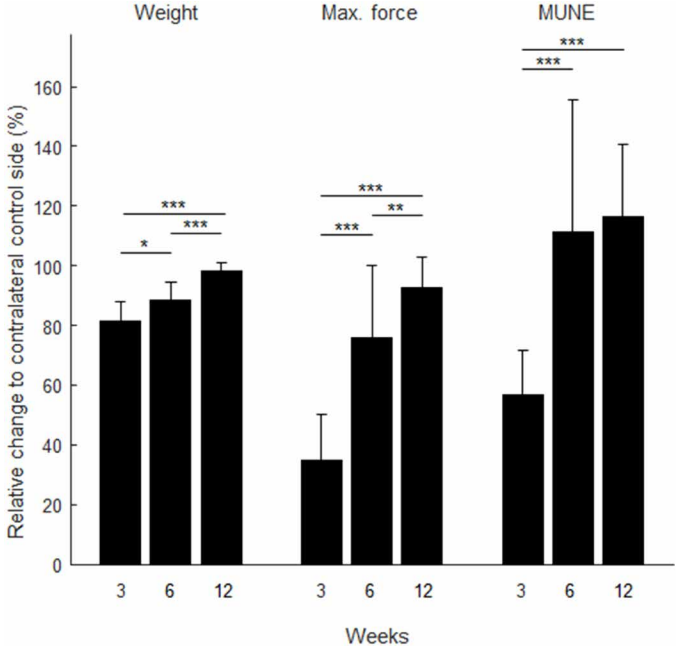

Fig. 5. Functional and structural muscle analyses. Muscle weight, force, and motor unit number estimations (MUNEs) significantly increased between weeks 3 and 12 (ANCOVA, $P < 0.0001$), indicating a progressive reinnervation of the target muscle after the nerve transfer. Muscle force was low (34.98 ± 15.45%, $n = 10$) compared with the contralateral control side at 3 weeks, but significantly increased to 75.87 ± 24.39% ($n = 11$) at 6 weeks (ANCOVA, $^{***}P < 0.001$) and to 92.57 ± 10.15% ($n = 9$) from 6 to 12 weeks (ANCOVA, $^{**}P = 0.006$). Muscle mass initially decreased to 81.38 ± 6.52% because of denervation compared with control at 3 weeks ($n = 14$) but increased to 88.25 ± 6.40% ($n = 13$) at 6 weeks and to 98.18 ± 2.95% ($n = 14$) at 12 weeks. The differences between weeks 3 and 6 and between weeks 6 and 12 were both significant (ANCOVA, $^{*}P = 0.014$ and $^{***}P < 0.0001$, respectively). Motor units increased from 56.62 ± 14.87% ($n = 10$) compared with control at 3 weeks, to 111.22 ± 44.58% ($n = 11$) at 6 weeks, and 116.31 ± 24.50% ($n = 9$) at 12 weeks. Differences between weeks 3 and 6 were statistically significant (ANCOVA, $^{***}P < 0.0001$).

is evident from the motor unit analyses (Fig. 5), within 6 weeks, over 100% of the motor unit population was restored and hyperreinnervation was present, which is typically not the case in primary repairs. From a clinical perspective, these results explain the excellent functional outcomes of nerve transfers even after long muscular denervation periods in biological reconstructions and TMR (*16*–*18*). Therefore, surgical reconstruction should aim at transferring donor nerves with large motor unit pools close to the target muscle to minimize regeneration distance and maximize the functional outcome.

Neuroma treatment and surgical refinement of nerve transfers

The surplus of motor neurons that did not reinnervate muscle fibers contributed to the formation of neuromas at the insertion of the nerve into the muscle. This presumably resulted from motor axons not finding sufficient neurotrophic support for making permanent contact with neuromuscular junctions, representing the axonal surplus exceeding the muscle's innervation capacity. In addition, sensory axons that contribute to most of the ulnar nerve presumably formed the largest portion of this neuroma, as they did not find a relevant target organ, e.g., denervated skin. However, previous studies have shown that transferring nerves after neuroma resection into intact muscle leads to the formation of atypical intramuscular neuromas without the typical pain (*19*) and that intramuscular translocation or TMR is instead a viable treatment option for treating painful neuromas (*20*). With further knowledge on the optimal donor-to-recipient ratio in nerve transfers, these procedures can be additionally refined to specifically transfer the exact number of axons that a target muscle can accept and therefore enable additional nerve transfers.

Hyper-reinnervation of the target muscle

Most nerve transfer procedures extract predominant motor fascicles from multifascicular nerves with a greater number of axons of distal targets. Thus, the target muscle is potentially reinnervated by a

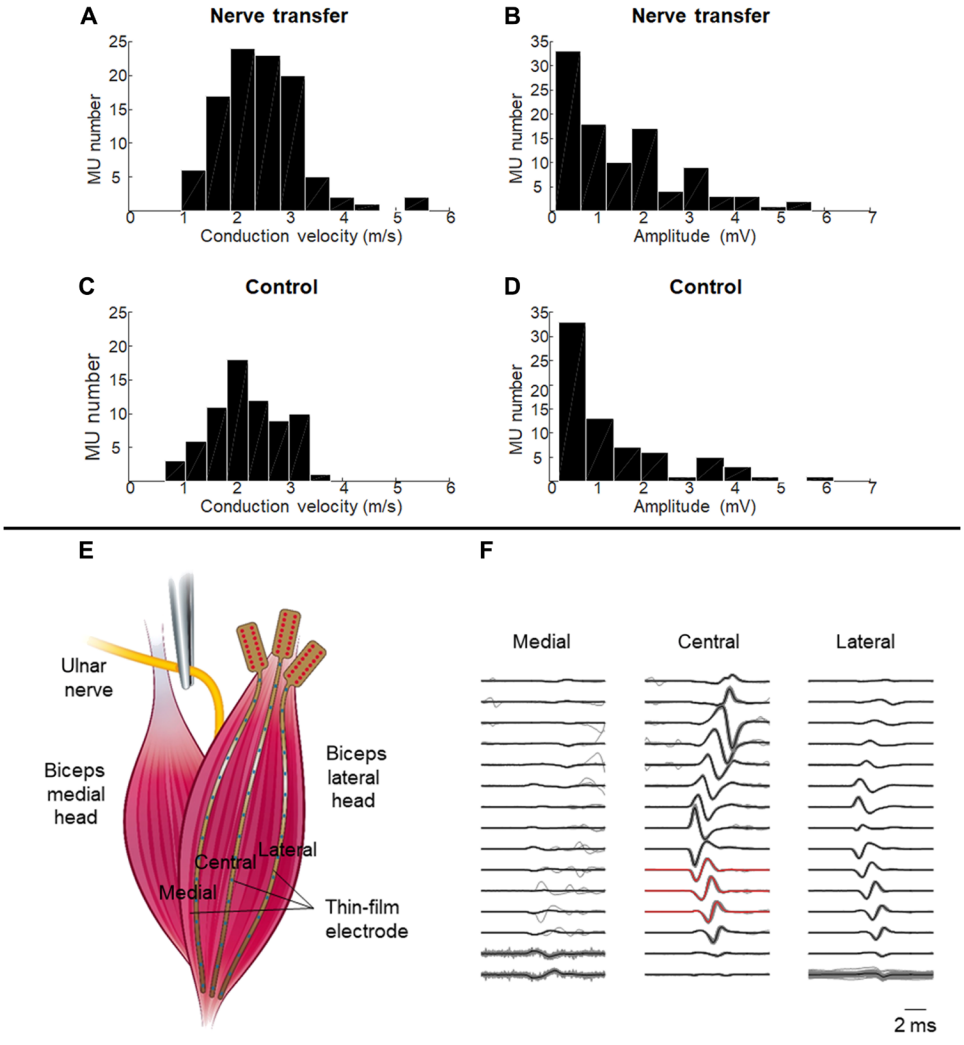

Fig. 6. Electrophysiological muscle analyses. Histograms of the muscle fiber conduction velocity (MFCV) and motor unit action potential amplitude for the reinnervated (**A** and **B**) and control (**C** and **D**) sides. Data from nine animals are pooled together (100 and 70 motor units were detected from the nerve transfer and control sides, respectively; no motor unit action potentials were observed for two animals in the control side). Greater conduction velocity was observed following the nerve transfer [2.50 ± 0.86 m/s versus 2.25 ± 0.75 m/s; $P = 0.017$, mixed model analysis, Gaussian distribution (A and C)]. For both groups, the amplitude distribution was skewed (B and D), and the linear mixed model was applied to the logarithmic values of the amplitude. The amplitude was not affected by the nerve transfer ($P = 0.15$, linear mixed model analysis). (**E**) Epimysial high-density EMG signals were recorded with multichannel electrode arrays with 16 oval detection sites (140 μm by 40 μm) with 1-mm intersite distance from the biceps lateral head muscle. Three arrays were applied over the epimysium along the muscle fibers, and asynchronous motor unit activity was induced by sequential crushes of the ulnar nerve in the reinnervated side, as represented in this figure (or the musculocutaneous nerve in the control side). (**F**) Action potentials generated by the same motor unit (gray traces) were averaged (black traces) and characterized by the conduction velocity. Two to four channels with clear propagating components (red traces) were selected to calculate the propagation delay. Conduction velocity was obtained as the ratio between the intersite distance and the propagation delay. In the representative example shown in this figure, the conduction velocity calculated from the three selected channels from the central electrode was 2.01 m/s. MU, motor unit.

higher axonal input. This is a consequence of a large number of axons competing for the reinnervation of a limited number of muscle fibers and results in smaller muscle units, i.e., fewer fibers per motor neuron. In our analyses, we could show that a high-capacity agonistic nerve transfer is able to hyper-reinnervate a single target muscle. This hyper-reinnervation was shown structurally by retrograde labeling of the motor units innervating the target muscle and functionally by progressive electrostimulation. Furthermore, we functionally evaluated muscle units using high-density epimysial recordings, which indicated that the largest muscle units with greater conduction velocities were fractioned after the nerve transfer so that more motor axons innervated smaller muscle units with larger conduction velocities. Overall, this suggests that the target muscle is reinnervated by a substantially greater number of motor neurons to form smaller contractile muscle units than with its physiological innervation.

Changes in the target muscle properties

Motor units have aligned physiological properties as a result of neonatal motor unit maturation (*21*). Following the nerve transfer, the targeted muscle fibers were reinnervated by motor neurons with different physiological properties, which led to a change in MHC expression in the targeted muscle fibers. The resulting muscle fiber population was similar to muscles physiologically innervated by the ulnar nerve, such as the intrinsic muscles. Hence, the reinnervating

motor neurons changed the targeted muscle fiber protein expression. This is presumably a consequence of motor unit hierarchy (*22*), where motor neurons govern MHC expression in reinnervated muscle fibers, as it has been previously shown in cross-reinnervation experiments (*23*, *24*). Therefore, surgically connecting axons of motor neuron pools of lost distal muscles to proximal stump muscles in amputees modifies the target muscle fiber composition. The targeted muscle fibers become physiologically similar to the originally innervated muscle, but in an anatomically different place. Hereby, it is possible to rewire the intact spinal control structures of amputated hand muscles to the remaining proximal muscles in the amputee's stump, thus providing a bioscreen with physiologically similar biosignals of the lost hand.

Target muscle as a bioscreen of neural activity

Overall, our analyses suggest that target muscles are able to accept structural and functional hyper-reinnervation following nerve transfers. Patients treated with nerve transfers could therefore possibly recruit more motor units to a finer degree in the targeted muscles. This is in agreement with a previous human study that showed smaller muscle units when pectoralis muscles were reinnervated with high-capacity nerve transfers following TMR surgery (*6*). These effects could be used for prosthetic control, as the target muscle can serve as a biological amplifier of spinal motor neuron activity, as we have shown previously (*9*). Following this concept, TMR recreates the central and peripheral conditions that are lost with the amputation by transforming targeted muscle fibers and grouping them in smaller units with presumably finer control. It is therefore, in principle, possible to recreate the neural and muscular conditions of an amputated donor nerve in a targeted muscle. Furthermore, a recent functional magnetic resonance imaging study has shown that after amputation, the corresponding motor cortex regions of the extremity are initially lost but restored after TMR (*25*). Therefore, surgical rewiring of peripheral nerves restores motor unit integrity by changing target muscles with excellent regeneration properties and is likely to restore the central pathways required for dexterous extremity control. As it is anatomically possible to surgically rewire multiple donor nerves to the remaining proximal muscles in all amputation levels of the upper extremity, we can potentially offer this concept to a variety of patients (*8*, *18*, *26*).

CONCLUSION

In summary, the results of this study illustrate that motor units adapt to surgical rewiring. Nerve transfers, as used in TMR, lead to highly functional muscle reinnervation and change the motor unit composition with respect to function and structure. In conclusion, we have shown that nerve transfers can be used to rewire target muscles to different spinal areas that subsequently adapt to the properties of the nerves' original muscles. This structural and functional rewiring can be applied for both biological and prosthetic extremity reconstructions and may help to restore dexterous extremity control and thereby limit the lifetime burden of afunctional extremities (*9*).

MATERIALS AND METHODS

Animals

Sixty-six Sprague-Dawley rats (male, aged 8 to 10 weeks) were allocated to muscle analyses or retrograde labeling. For muscle analyses, animals were allocated into three groups to analyze muscle weight, muscle force, and MUNE after the transfer of the ulnar nerve to the lateral head of the biceps muscle after 3, 6, or 12 weeks, respectively. In the retrograde labeling trial, 21 animals were allocated to quantify motor neurons via retrograde labeling of either the ulnar nerve ($n = 6$) or the biceps' lateral head without nerve transfer ($n = 6$) or 12 weeks after the nerve transfer ($n = 9$). In addition, in 15 Thy1-GFP rats [male, aged 8 to 10 weeks (*27*, *28*)], the muscular reinnervation was visualized with ($n = 6$) or without ($n = 9$) nerve transfer surgery. In addition, target muscles were analyzed with epimysial multichannel EMG electrodes in nine animals 12 weeks after the nerve transfer surgery. In the nerve transfer groups, the contralateral extremity was used as an internal control in all the analyses. All animals received humane care in compliance with the principles of laboratory animal care as recommended by the FELASA (Federation for Laboratory Animal Science Associations) (*29*). Experimental planning, conduction of experiments, and reporting were done according to the ARRIVE (Animal Research: Reporting of In Vivo Experiments) guidelines (*30*). Approval was obtained from the ethics committee of the Medical University of Vienna and the Austrian Ministry for Research and Science (reference number BMWF-66.009/0222-WF/II/3b/2014).

Selective nerve transfer model

Nerve transfers were performed as previously described (Fig. 1A) (*31*). In brief, an incision was made on the upper extremity from the pectoral muscle to the medial epicondyle of the humerus. Using a surgical microscope, the ulnar nerve was exposed and cut proximal to the medial epicondyle. First, the biceps' lateral head was denervated by resection of the motor branch to prevent any aberrant regenerative interaction. The ulnar nerve was neurotized to the epimysium of the motor branch's insertion point via two 11-0 (Ethilon, Ethicon, Johnson & Johnson Medical Care) sutures. Using this neurotization technique, the regeneration distance and, thus, the effect of denervation were kept to a minimum.

Muscle force testing and MUNEs

Maximum muscle force and MUNE were measured to analyze muscle innervation (*27*). Analyses were conducted bilaterally to compare the effects of the nerve transfer to the intact contralateral control side as a reference. The proximal tendon of the biceps muscle was folded into a loop and attached to a force transducer (BG-1000; Kulite Semiconductor Products, Leonia, NJ). The musculocutaneous nerve was cut, and the biceps' medial head was denervated to prevent any additional muscular contraction.

A shielded bipolar silver cuff electrode was used to apply electrical stimuli generated by a Grass S88 Stimulator (Grass Instrument Co., Quincy, MA). For the MUNE, the donor ulnar nerve was stimulated on the nerve transfer side, and the original motor branch was stimulated on the contralateral control side using 100-μs pulses at a rate of 0.5 Hz, with manually adjusted amplitude ranging from 0 to 10 V. The stimulation started with low enough amplitude to not elicit any force and was then gradually increased until the first motor unit produced a detectable force. Every time the force increased, the stimulus amplitude was held constant for 8 to 10 stimuli to average the force readings of the recruited motor unit. This procedure was repeated until 10 motor units were identified, and then the average force across the 10 motor units was calculated. For the maximum isometric tetanic force measurement, the nerve innervating the

biceps' lateral head was stimulated for 300 ms at increasing frequencies from 30 to 100 Hz and 2- to 6-V amplitude. The procedure was paused for 2 min after each set of stimuli set at the same amplitude to allow for muscle recovery. The maximum force was divided by the average motor unit force to estimate the total number of motor units. One animal from the 12-week's group had to be excluded because of premature decease during testing of the control side.

Epimysial high-density EMG analyses

MFCV was measured to investigate fiber diameter in the reinnervated muscle units (*32*). For this purpose, linear electrode arrays were placed along the muscle fiber direction to estimate the action potential propagation delay. Specifically designed multichannel thin-film EMG electrodes were used, consisting of a 20-μm-thick polyimide substrate with 16 linearly arranged detection sites with 1-mm intersite distance (Fig. 6E) (*33*). The size and flexibility of the electrodes allowed their application directly on the muscle surface to record epimysial signals for MFCV estimation. Three thin-film electrodes were placed longitudinally to cover the medial, central, and lateral portions of the muscle (Fig. 6E). Asynchronous motor unit activity was obtained by crushing the ulnar nerve in the reinnervated side and the musculocutaneous nerve in the control side sequentially from proximal to distal. EMG activity was recorded in a monopolar mode with a multichannel EMG amplifier (EMG-USB2, OT Bioelettronica, Torino, Italy) at 10,240-Hz sampling rate and with 12-bit resolution. Signals were amplified with a gain in the range 500 to 1000 and bandpass filtered between 100 and 4400 Hz. The procedure was conducted on both the reinnervated and control sides of each animal. Signals were decomposed into the constituent motor unit action potentials using the EMGLAB software (*34*). Single differential bipolar signals were obtained from the recordings before decomposition to eliminate artifacts. Action potentials generated by the same motor unit were averaged to obtain a multichannel template. Each motor unit was characterized by the amplitude of its action potential and by MFCV. The amplitude inversely depends on the distance between the motor unit territory and the detection site (*35*). The innervation zone was identified from the bipolar signals as the zone where the waveform polarity changed. A set of two to four single differential channels with dominant propagating components were identified proximally or distally to the innervation zone for the estimation of MFCV (Fig. 6, E and F). MFCV was estimated as the ratio between the action potential propagation delay along the selected channels and the intersite spacing (1 mm) using the algorithm proposed in (*36*). The action potential amplitude corresponding to each motor unit was calculated as the peak-to-peak highest monopolar amplitude among the channels with dominant propagating components.

Muscle analyses

Muscle weight was analyzed to assess the effects of denervation, and the whole biceps was removed for histological analysis. Both analyses were performed on the treated and contralateral biceps to serve as a control. After completion of the maximum muscle force and the MUNE protocol, biceps muscles were carefully dissected, tendons were removed, and weight was assessed using a microscale. Afterward, muscles were embedded in O.C.T. compound (Tissue-Tek, Sakura Finetek, CA, USA), frozen in liquid nitrogen–cooled isopentane, and stored at −80°C for a minimum of 24 hours. The effect of the nerve transfer on fiber populations was analyzed using an immunohistochemistry protocol against MHC subtypes (*37*, *38*). Modifications were made for better contrast and automated analyses as previously described (*39*, *40*). Full cross-sectional samples with a width of 20 μm were stained with a primary antibody cocktail of phosphate-buffered saline (PBS) with 10% goat serum containing MHC-I (BA-F8; 1:50), MHC-IIa (SC-71; 1:600), and MHC-IIb (BF-F3; 1:100) antibodies for 60 min [Developmental Studies Hybridoma Bank (DSHB), Iowa, USA]. PBS containing 10% goat serum was used as a blocking buffer. PBS with 10% goat serum was mixed with secondary antibodies against Alexa Fluor 633 immunoglobulin G2b (IgG2b) (1:250), Alexa Fluor 488 IgG1 (1:250), and Alexa Fluor 555 IgM (1:250) and applied for 60 min (Life Technologies, CA, USA). Per animal, the entire muscle's cross section was analyzed using an automated analyses protocol as previously described (*39*, *40*).

Muscle innervation and neuromuscular junctions

The structural reinnervation of the nerve transfer and the consecutive formation of the neuromuscular junctions were assessed in muscles of Thy1-GFP rats (*28*). First, muscles were cut longitudinally at a width of 300 μm from medial to lateral. Samples were washed three times for 10 min using phosphate buffered saline with triton (PBST) and blocked for 2 hours with blocking buffer (PBST with 10% goat serum and 1% bovine serum albumin). A conjugate of α-bungarotoxin and Alexa Fluor 594 (cat. no. B-13423, Life Technologies) was diluted (1:100) in blocking buffer and applied for 16 hours to the slides. Last, the slides were covered with fluorescent mounting medium (Dako, Austria) and coverslips. Slides were imaged using a Leica confocal and multiphoton microscope with two spectral windows for GFP and Alexa Fluor 594. Three-dimensional stacks were acquired to investigate the reinnervation of the lateral head of the biceps and the formation of neuromuscular junctions. Innervation was confirmed by observing the overlapping of green fluorescence from the axons expressing GFP and the red fluorescence of stained neuromuscular junctions. The entire reinnervation zone was analyzed, including several adjacent cross sections, until no neuromuscular junctions were present.

Retrograde labeling

Changes in the number of motor neurons in the spinal cord following the nerve transfer surgery were assessed using retrograde labeling. Motor neurons were labeled using 5% Fluoro-Ruby (Invitrogen, Carlsbad, CA), as previously described (*41*). In six control animals, the number of motor neurons innervating the ulnar nerve was analyzed by transecting it at two-thirds of the humerus and staining it for 60 min in a well filled with retrograde tracer. The number of motor neurons innervating the biceps' lateral head was evaluated in six control animals and nine animals 12 weeks after the nerve transfer. Using a Hamilton microsyringe, 10 μl of retrograde tracer was injected evenly into the lateral head. Care was taken to prevent any leakage from the muscle, and the needle was left in place for 2 min before slow withdrawal. One week after the retrograde labeling, the animals were deeply anesthetized, followed by a left ventricular perfusion with 200 ml of warmed PBS and afterward 400 ml of 4% paraformaldehyde (PFA) in PBS. Then, the spinal cord segments C4-Th1 were harvested, stored in 4% PFA for 24 hours, and frozen in Tissue-Tek. The spinal cord was cut into 50-μm longitudinal sections using a cryostat (Leica, Germany). In each spinal cord section, the number of labeled motor cell bodies was counted under a fluorescence microscope (×100 magnification; Nikon). Quantification was done by one trained observer blinded to the experimental groups.

Statistical analyses

The primary outcome experimental parameter for functional muscle testing was muscle force. The secondary outcomes were MUNE and muscle weight. All variables were measured for three different groups (measures at weeks 3, 6, and 12, respectively) both on the treated (left) and on the untreated (right) sides. For the ratios between the treated and untreated sides, we provided means and 95% confidence intervals for each group. Differences between groups were tested with ANCOVA, considering the untreated side as a covariate. All presented P values for pairwise comparisons were not corrected for multiple testing because when planning this trial already, we considered a hierarchical testing strategy: to first consider the comparison between weeks 3 and 12 and then to consider the remaining two pairwise comparisons only if this difference is significant. Concerning the distribution of fiber types, we reported the average percentage, the average number of a specific fiber, and the corresponding SD. Conduction velocity is known to have a Gaussian distribution. The Lilliefors test was used to confirm this hypothesis. To analyze the difference between the treated and the control sides in MFCV and the amplitude, we applied linear mixed models with the rat identifier as random factor using SAS PROC MIXED.

REFERENCES AND NOTES

1. C. J. Heckman, R. M. Enoka, Motor unit. *Compr. Physiol.* **2**, 2629–2682 (2012).
2. S. Y. Fu, T. Gordon, The cellular and molecular basis of peripheral nerve regeneration. *Mol. Neurobiol.* **14**, 67–116 (1997).
3. J. E. Totosy de Zepetnek, H. V. Zung, S. Erdebil, T. Gordon, Innervation ratio is an important determinant of force in normal and reinnervated rat tibialis anterior muscles. *J. Neurophysiol.* **67**, 1385–1403 (1992).
4. C. Oberlin, D. Béal, S. Leechavengvongs, A. Salon, M. C. Dauge, J. J. Sarcy, Nerve transfer to biceps muscle using a part of ulnar nerve for C5–C6 avulsion of the brachial plexus: Anatomical study and report of four cases. *J. Hand Surg.* **19**, 232–237 (1994).
5. J. A. Bertelli, J. C. Mira, M. Pecot-Dechavassine, A. Sebille, Selective motor hyperreinnervation using motor rootlet transfer: An experimental study in rat brachial plexus. *J. Neurosurg.* **87**, 79–84 (1997).
6. T. Kapelner, N. Jiang, A. Holobar, I. Vujaklija, A. D. Roche, D. Farina, O. C. Aszmann, Motor unit characteristics after targeted muscle reinnervation. *PLOS ONE* **11**, e0149772 (2016).
7. O. C. Aszmann, A. D. Roche, S. Salminger, T. Paternostro-Sluga, M. Herceg, A. Sturma, C. Hofer, D. Farina, Bionic reconstruction to restore hand function after brachial plexus injury: A case series of three patients. *Lancet* **385**, 2183–2189 (2015).
8. T. A. Kuiken, L. A. Miller, R. D. Lipschutz, B. A. Lock, K. Stubblefield, P. D. Marasco, P. Zhou, G. A. Dumanian, Targeted reinnervation for enhanced prosthetic arm function in a woman with a proximal amputation: A case study. *Lancet* **369**, 371–380 (2007).
9. D. Farina, I. Vujaklija, M. Sartori, T. Kapelner, F. Negro, N. Jiang, K. Bergmeister, A. Andalib, J. Principe, O. C. Aszmann, Man/machine interface based on the discharge timings of spinal motor neurons after targeted muscle reinnervation. *Nat. Biomed. Eng.* **1**, 0025 (2017).
10. T. A. Kuiken, D. S. Childress, W. Z. Rymer, The hyper-reinnervation of rat skeletal muscle. *Brain Res.* **676**, 113–123 (1995).
11. B. Gesslbauer, L. A. Hruby, A. D. Roche, D. Farina, R. Blumer, O. C. Aszmann, Axonal components of nerves innervating the human arm. *Ann. Neurol.* **82**, 396–408 (2017).
12. W. Z. Ray, J. Chang, A. Hawasli, T. J. Wilson, L. Yang, Motor nerve transfers: A comprehensive review. *Neurosurgery* **78**, 1–26 (2016).
13. J. B. Hursh, Conduction velocity and diameter of nerve fibers. *Am. J. Physiol.* **127**, 131–139 (1939).
14. E. Henneman, C. B. Olson, Relations between structure and function in the design of skeletal muscles. *J. Neurophysiol.* **28**, 581–598 (1965).
15. X. Hu, W. Z. Rymer, N. L. Suresh, Motor unit pool organization examined via spike-triggered averaging of the surface electromyogram. *J. Neurophysiol.* **110**, 1205–1220 (2013).
16. J. A. Bertelli, M. F. Ghizoni, Selective motor hyperreinnervation by using contralateral C-7 motor rootlets in the reconstruction of an avulsion injury of the brachial plexus. Case report. *J. Neurosurg.* **90**, 1133–1136 (1999).
17. T. A. Kuiken, G. A. Dumanian, R. D. Lipschutz, L. A. Miller, K. A. Stubblefield, The use of targeted muscle reinnervation for improved myoelectric prosthesis control in a bilateral shoulder disarticulation amputee. *Prosthet. Orthot. Int.* **28**, 245–253 (2004).
18. T. A. Kuiken, G. Li, B. A. Lock, R. D. Lipschutz, L. A. Miller, K. A. Stubblefield, K. B. Englehart, Targeted muscle reinnervation for real-time myoelectric control of multifunction artificial arms. *JAMA* **301**, 619–628 (2009).
19. A. L. Dellon, S. E. Mackinnon, Treatment of the painful neuroma by neuroma resection and muscle implantation. *Plast. Reconstr. Surg.* **77**, 427–438 (1986).
20. J. M. Souza, J. E. Cheesborough, J. H. Ko, M. S. Cho, T. A. Kuiken, G. A. Dumanian, Targeted muscle reinnervation: A novel approach to postamputation neuroma pain. *Clin. Orthop. Relat. Res.* **472**, 2984–2990 (2014).
21. R. L. Lieber, *Skeletal Muscle Structure, Function, and Plasticity* (Lippincott Williams & Wilkins, 2009).
22. A. J. Buller, J. C. Eccles, R. M. Eccles, Interactions between motoneurones and muscles in respect of the characteristic speeds of their responses. *J. Physiol.* **150**, 417–439 (1960).
23. K. I. Clark, T. P. White, Neuromuscular adaptations to cross-reinnervation in 12- and 29-mo-old Fischer 344 rats. *Am. J. Physiol.* **260**, C96–C103 (1991).
24. S. Schiaffino, C. Reggiani, Fiber types in mammalian skeletal muscles. *Physiol. Rev.* **91**, 1447–1531 (2011).
25. A. Serino, M. Akselrod, R. Salomon, R. Martuzzi, M. L. Blefari, E. Canzoneri, G. Rognini, W. van der Zwaag, M. Iakova, F. Luthi, A. Amoresano, T. Kuiken, O. Blanke, Upper limb cortical maps in amputees with targeted muscle and sensory reinnervation. *Brain* **140**, 2993–3011 (2017).
26. O. C. Aszmann, I. Vujaklija, A. D. Roche, S. Salminger, M. Herceg, A. Sturma, L. A. Hruby, A. Pittermann, C. Hofer, S. Amsuess, D. Farina, Elective amputation and bionic substitution restore functional hand use after critical soft tissue injuries. *Sci. Rep.* **6**, 34960 (2016).
27. S. W. P. Kemp, P. D. Phua, K. N. Stanoulis, M. D. Wood, E. H. Liu, T. Gordon, G. H. Borschel, Functional recovery following peripheral nerve injury in the transgenic *Thy1-GFP* rat. *J. Peripher. Nerv. Syst.* **18**, 220–231 (2013).
28. A. M. Moore, G. H. Borschel, K. B. Santosa, E. R. Flagg, A. Y. Tong, R. Kasukurthi, P. Newton, Y. Yan, D. A. Hunter, P. J. Johnson, S. E. Mackinnon, A transgenic rat expressing green fluorescent protein (GFP) in peripheral nerves provides a new hindlimb model for the study of nerve injury and regeneration. *J. Neurosci. Methods* **204**, 19–27 (2012).
29. J. Guillen, FELASA guidelines and recommendations. *J. Am. Assoc. Lab. Anim. Sci.* **51**, 311–321 (2012).
30. C. Kilkenny, W. J. Browne, I. C. Cuthill, M. Emerson, D. G. Altman, Improving bioscience research reporting: The ARRIVE guidelines for reporting animal research. *PLOS BIOL.* **8**, e1000412 (2010).
31. K. D. Bergmeister, M. Aman, O. Riedl, K. Manzano-Szalai, M. E. Sporer, S. Salminger, O. C. Aszmann, Experimental nerve transfer model in the rat forelimb. *Eur. Surg.* **48**, 334–341 (2016).
32. T. Sadoyama, T. Masuda, H. Miyata, S. Katsuta, Fibre conduction velocity and fibre composition in human vastus lateralis. *Eur. J. Appl. Physiol. Occup. Physiol.* **57**, 767–771 (1988).
33. S. Muceli, W. Poppendieck, F. Negro, K. Yoshida, K. P. Hoffmann, J. E. Butler, S. C. Gandevia, D. Farina, Accurate and representative decoding of the neural drive to muscles in humans with multi-channel intramuscular thin-film electrodes. *J. Physiol.* **593**, 3789–3804 (2015).
34. K. C. McGill, Z. C. Lateva, H. R. Marateb, EMGLAB: An interactive EMG decomposition program. *J. Neurosci. Methods* **149**, 121–133 (2005).
35. K. Roeleveld, D. F. Stegeman, H. M. Vingerhoets, A. Van Oosterom, The motor unit potential distribution over the skin surface and its use in estimating the motor unit location. *Acta Physiol. Scand.* **161**, 465–472 (1997).
36. D. Farina, W. Muhammad, E. Fortunato, O. Meste, R. Merletti, H. Rix, Estimation of single motor unit conduction velocity from surface electromyogram signals detected with linear electrode arrays. *Med. Biol. Eng. Comput.* **39**, 225–236 (2001).
37. D. Bloemberg, J. Quadrilatero, Rapid determination of myosin heavy chain expression in rat, mouse, and human skeletal muscle using multicolor immunofluorescence analysis. *PLOS ONE* **7**, e35273 (2012).
38. S. Ribarič, V. ČebaŠek, Simultaneous visualization of myosin heavy chain isoforms in single muscle sections. *Cells Tissues Organs* **197**, 312–321 (2013).
39. K. D. Bergmeister, M. Gröger, M. Aman, A. Willensdorfer, K. Manzano-Szalai, S. Salminger, O. C. Aszmann, Automated muscle fiber type population analysis with ImageJ of whole rat muscles using rapid myosin heavy chain immunohistochemistry. *Muscle Nerve* **54**, 292–299 (2016).
40. K. D. Bergmeister, M. Gröger, M. Aman, A. Willensdorfer, K. Manzano-Szalai, S. Salminger, O. C. Aszmann, A rapid automated protocol for muscle fiber population analysis in rat muscle cross sections using myosin heavy chain immunohistochemistry. *J. Vis. Exp.* e55441 (2017).
41. A. Hayashi, A. Moradzadeh, D. A. Hunter, D. H. Kawamura, V. K. Puppala, T. H. H. Tung, S. E. Mackinnon, T. M. Myckatyn, Retrograde labeling in peripheral nerve research: It is not all black and white. *J. Reconstr. Microsurg.* **23**, 381–389 (2007).

Acknowledgments: We thank A. Willensdorfer for excellent technical assistance throughout the project. In addition, we thank M. G. Urbanchek, P. Cederna, and their team for the help with the experimental design. The primary antibodies for MHC immunohistochemistry developed by S. Schiaffino were obtained from the DSHB, created by the NICHD of the NIH, and maintained at the Department of Biology, The University of Iowa. **Funding:** This work was supported by the Christian Doppler Research Association; Austrian Council for Research and Technology Development; Austrian Federal Ministry of Science, Research and Economy; and European Research Council (ERC) via the ERC Advanced Grant DEMOVE (no. 267888). None of the funding agencies were involved in the collection, analyses, and interpretation of data or writing and publication of this article. **Author contributions:** Conception and design: K.D.B., S.M., I.V., K.M.-S., E.U., R.A.B., C.S., O.R., F.F., G.H.B., D.F., and O.C.A. Analyses and interpretation of data: K.D.B., M.A., S.M., I.V., K.M.-S., E.U., R.A.B., C.S., O.R., S.S., F.F., G.H.B., D.F., and O.C.A. Drafting of the article: K.D.B., M.A., S.M., I.V., F.F., D.F., and O.C.A. Critical revision for important intellectual content and final approval of the version to be published: all authors. **Competing interests:** The authors declare that they have no competing interests. **Data and materials availability:** All data needed to evaluate the conclusions in the paper are present in the paper. Additional data related to this paper may be requested from the authors.

Submitted 26 May 2018
Accepted 26 November 2018
Published 2 January 2019
10.1126/sciadv.aau2956

Citation: K. D. Bergmeister, M. Aman, S. Muceli, I. Vujaklija, K. Manzano-Szalai, E. Unger, R. A. Byrne, C. Scheinecker, O. Riedl, S. Salminger, F. Frommlet, G. H. Borschel, D. Farina, O. C. Aszmann, Peripheral nerve transfers change target muscle structure and function. *Sci. Adv.* **5**, eaau2956 (2019).

Peripheral nerve transfers change target muscle structure and function

Konstantin D. Bergmeister, Martin Aman, Silvia Muceli, Ivan Vujaklija, Krisztina Manzano-Szalai, Ewald Unger, Ruth A. Byrne, Clemens Scheinecker, Otto Riedl, Stefan Salminger, Florian Frommlet, Gregory H. Borschel, Dario Farina and Oskar C. Aszmann

Sci Adv **5** (1), eaau2956.
DOI: 10.1126/sciadv.aau2956